Effective Exploitation of Ambient EM Energy for Driving Emerging IoT Devices: Case Study

Kamila Shalpeneyeva, Kassen Dautov, Mohammad Hashmi, and Galymzhan Nauryzbayev(✉)

School of Engineering and Digital Sciences, Nazarbayev University, Astana 010000, Kazakhstan
{kamila.shalpeneyeva,kassen.dautov,mohammad.hashmi, galymzhan.nauryzbayev}@nu.edu.kz

Abstract. Radio-frequency (RF) energy harvesting-enabled sensor nodes can alleviate the charging challenges by exploitation of electromagnetic waves in the ambient proximity and contribute to more efficient use of energy resources that is essential to deploy numerous Internet-of-Things (IoT) nodes. An RF spectrum survey was conducted at Nazarbayev University campus to discover potential RF energy sources and their available power levels which revealed four prospective frequency bands. Consequently, two frequencies that demonstrated sufficient power levels and stability for an efficient RF energy harvesting were selected from the analysis of a full week data measurements. Then, the rectangular patch microstrip-fed dual-band antenna operating on those frequencies was designed and fabricated. The proposed meander-line antenna design allowed miniaturization of the effective surface area that is useful for IoT sensor applications. The fabricated prototype and simulation measurements were in good agreement.

Keywords: Energy harvesting (EH) · Internet-of-Things (IoT) · multi-band antenna · radio-frequency (RF) spectral survey

1 Introduction

The rapid growth and development of an Internet-of-Things (IoT) infrastructure are leading to the increase in a number of sensor nodes in wireless networks [1]. The extensive deployment of IoT networks has led to exploring complications of battery charging and high maintenance cost of numerous devices [2]. Therefore, wireless charging approaches, that enable maintenance-free sensor nodes, became more attractive in comparison to the conventional battery charging techniques [1,3,4]. The advancement and extensive use of wireless communication

This research was funded by Nazarbayev University under Collaborative Research Program Grants #11022021CRP1513 (G. Nauryzbayev) and #021220CRP0222 (M. Hashmi).

K. Rabie et al. (Eds.): IoTaaS 2022, LNICST 506, pp. 48–57, 2023.
https://doi.org/10.1007/978-3-031-37139-4_5

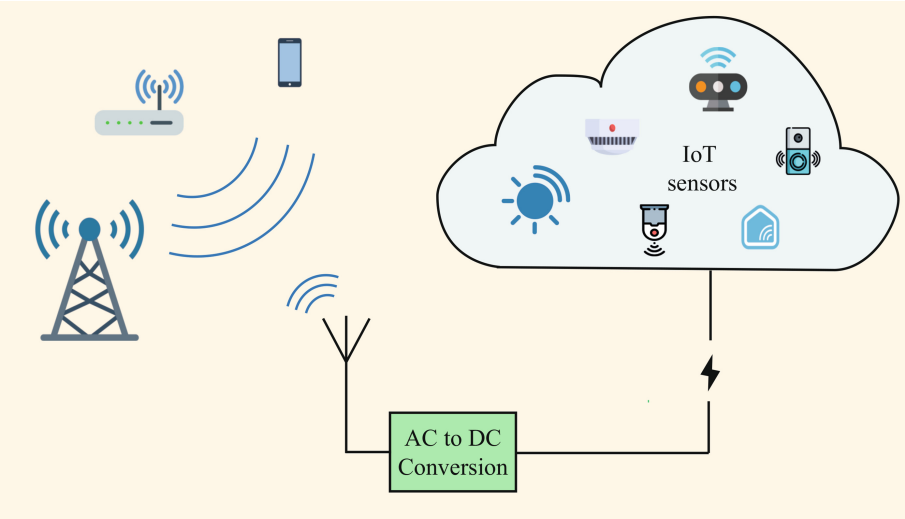

Fig. 1. Exploitation of EM pollution for wireless charging.

have made urban areas crowded with a myriad of user devices, Wi-Fi routers, cell phones, and sensors emitting electromagnetic (EM) waves that saturate the environment with radio-frequency (RF) energy [5]. The wireless devices emit the EM waves to communicate with each other, however, indeed only a fragment of that energy is processed for information decoding while the remaining part freely flows polluting the environment [6]. Considering the inevitability of this, the unused energy in an ambient environment could be utilized to satisfy the charging requirements of ultra low-power devices [3,7]. This could enable the deployment of autonomous IoT sensor networks. Recycling the unused EM waves contributes toward achieving the green communication paradigm through RF energy harvesting (EH) [8–10].

Available RF signal power needs to be determined and quantified to design and implement an effective EH system. This has been reportedly achieved by conducting spectrum surveys, one of which emphasized that maximum signals' power levels are more informative measurement rather than their density [11]. The measurements reported in [12,13] considered the conditions of a location, time and possible effects they had on the acquired results recognizing varying RF energy presence with respect to those conditions. An initial step of RF EH is antenna design that is tuned to operate within certain bands. Owing to the low-power levels of available RF signals, it would be beneficial to have a few sources to harvest from. Previous works have reported dual-band [14–16] and multi-band [9,17] antenna for RF EH applications.

In an aim to address the above-mentioned need, this paper proposes to realize simultaneous RF energy harvesting from multiple energy carriers. Keeping this in a perspective, an RF spectrum survey was performed on the campus of Nazarbayev University (NU, Astana, Kazakhstan) to determine the frequency

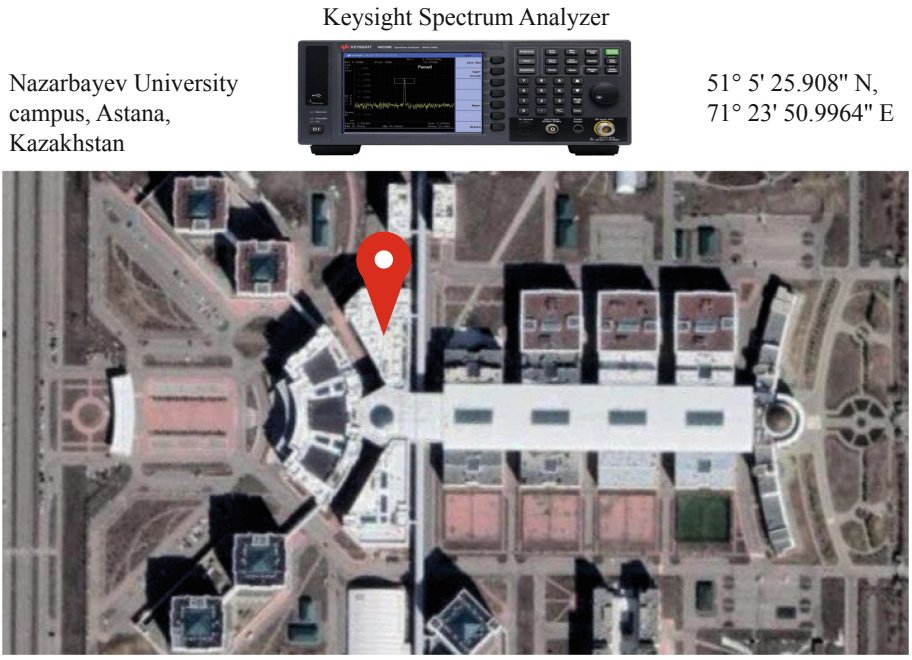

Fig. 2. Location of spectrum analyzer for RF survey (from the Google Maps).

bands eligible for efficient RF EH. The location of the RF spectrum survey represented a customary public place where an IoT network would likely be installed. This allowed estimating the potential for EH of the site from the taken data measurements. As a result, two frequencies of 1.74 GHz and 2.4 GHz were selected as prominent sources demonstrating the power levels above −30 dBm throughout the data measurement period. A dual-band antenna of a miniaturized size operating at those frequencies was designed and experimentally validated.

This paper is organized as follows. Section 2 introduces the proposed model of exploitation of EM pollution for IoT sensors powering. In addition, it provides a basis for conducting an RF spectral survey with observed measurements. Section 3 describes the design approach, simulation and experimental validation results of the dual-band antenna. Sections 4 and 5 cover the discussion of the results and conclusion of this paper, respectively.

2 Ambient RF Measurements

Nowadays, wireless networks are strongly packed with various devices communicating through RF signals. As a consequence, the areas with such networks have a lot of freely roaming EM waves that are not used for data transfer. Figure 1 depicts a scenario of the crowded network with RF signals available for EH. Ambient RF energy can be therefore recycled and used to power IoT sensors

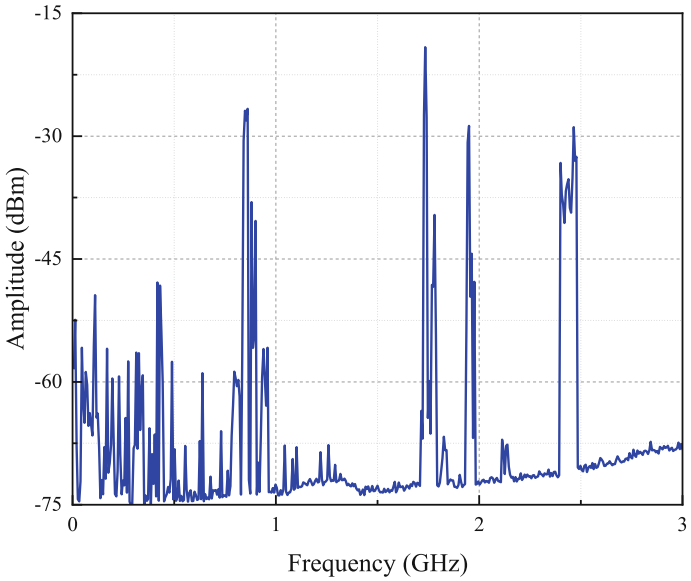

Fig. 3. The measured RF spectrum.

that require small amounts of energy. This option is a promising approach to enable independent IoT devices and contribute toward the green communication. The first step of collecting unused EM waves is capturing the signals with a dedicated antenna optimized to the present frequencies in that proximity. Moreover, the proper design of the EH system requires identifying the feasible spectral bands for RF harvesting. The signal with peak power above −30 dBm is treated as a prominent source for RF EH [11].

2.1 Methodology

To approach realizing efficient RF EH, it was necessary to determine the present frequency bands and their power levels. This was achieved by conducting an RF spectrum survey over a period of time to establish the power availability and consistency. The survey location was the NU campus, as illustrated in Fig. 2. The measurements were conducted during the working hours from 9 a.m. to 6 p.m. in a period of one week assuming that RF signals were more active during the daytime. The equipment used was the Keysight N9320B Spectrum Analyzer operating between 9 kHz−3 GHz. The resolution bandwidth was 100 kHz, the attenuation was set at 5 dB to avoid a compression of small signals [12]. The antenna used for signal capturing had a broad bandwidth of 800 MHz−8 GHz. The measurement setup recorded the maximum available peaks of incoming signals throughout the average day.

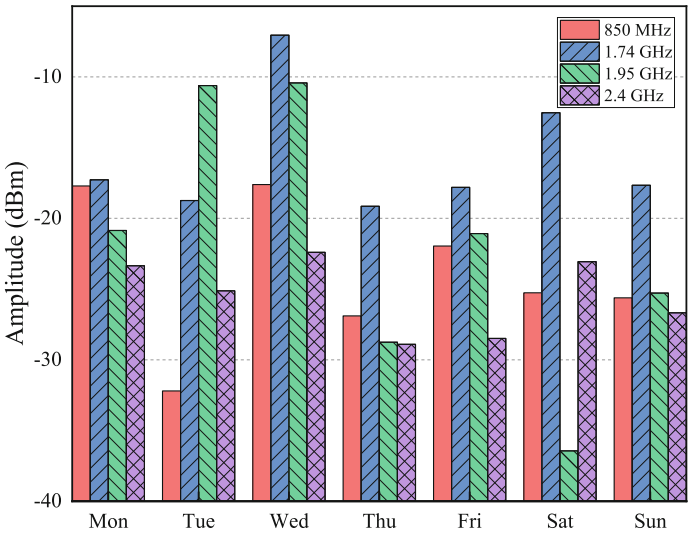

Fig. 4. The measured maximum power: power level vs week days.

2.2 Obtained Results and Analysis

As a result of the spectral survey at NU, multiple active frequency bands were observed to persist consistently in a period of the taken measurements. Figure 3 demonstrates the RF spectrum recorded on an average day. It is apparent that there are four main frequency peaks that are centered at 850 MHz, 1.74 GHz, 1.95 GHz, and 2.4 GHz which stand for the GSM (Global System for Mobile) and Wi-Fi bands. These frequency bands were measured and analyzed during a period of one week. Figure 4 depicts the maximum power levels of four distinguished bands that were recorded on each day of the week. As depicted, 1.74 GHz frequency signal demonstrated the highest activity throughout the week with a power level above −20 dBm at all times peaking at −6 dBm. Similarly, 2.4 GHz signal showed a stable trend with power level fluctuating between −20 dBm and −30 dBm. In general, the other two frequency bands showed potential for EH feasibility by having power levels within −20 dBm and −30 dBm during most days but were below the minimum power threshold of −30 dBm. Therefore, the two most active and stable frequencies of 1.74 GHz and 2.4 GHz were chosen for RF EH at the NU campus. For this purpose, the dual-band antenna was designed which is thoroughly described in Sect. 3.

3 Dual-Band Antenna Design

As stated above, simultaneous RF EH from two frequencies is realized by a means of a dual-band antenna. The rectangular patch antenna was selected due to its easy and low-cost fabrication. Figure 5 shows the antenna of dimensions 50×35

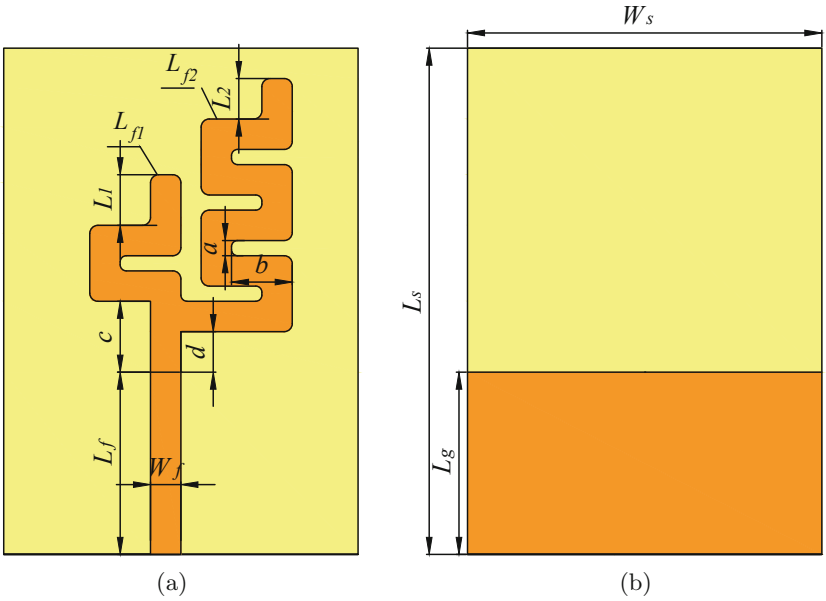

Fig. 5. The dual-band antenna structure: (a) top view (b) bottom view.

Table 1. The final optimized antenna parameters.

Parameter	W_s	L_s	W_f	L_g	a	b	c	d	L_1	L_2
Value (mm)	35	50	3	18	1.5	6	7	4	3.2	7

mm which was designed in CST Studio Suite. The meander-line approach that allows minimizing the surface area was chosen to shape the radiating element. The antenna's radiating patch comprises two meander lines each corresponding to a single resonant frequency. The lengths of line segments were calculated to be $\lambda/4$ of the resonant frequency and tuned to the desired values of 1.74 GHz and 2.4 GHz. Figure 7(a) depicts a single meander line (L_{f_1}) response, while Fig. 7(b) illustrates obtaining dual-band characteristic by adding a second meander line (L_{f_2}) to the radiating element. The microstrip feed line was calculated to have a characteristic impedance of 50-Ω with (1) and (2).

$$L_f = \frac{\lambda_0}{4\sqrt{\epsilon_{eff}}}, \tag{1}$$

$$Z_0 = \begin{cases} \frac{60}{\sqrt{\epsilon_{eff}}} \ln\left[\frac{8h}{W_f} + \frac{W_f}{4h}\right], & \frac{W_f}{h} \leq 1, \\ \frac{120\pi}{\sqrt{\epsilon_{eff}}\left[\frac{W_f}{h} + 1.393 + 0.667\right] \ln\left[\frac{W_f}{h} + 1.444\right]}, & \frac{W_f}{h} > 1. \end{cases} \tag{2}$$

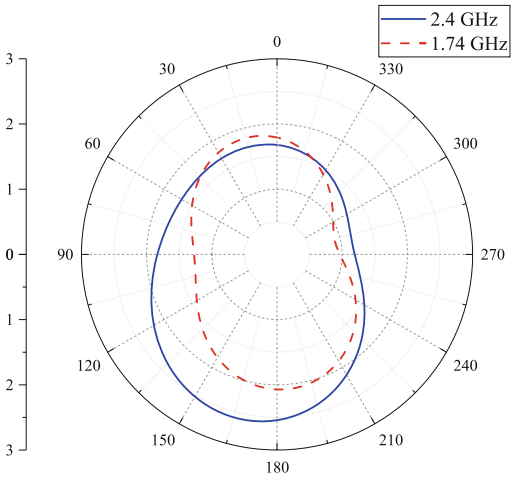

Fig. 6. 3D radiation pattern: (a) 1.74 GHz; (b) 2.4 GHz.

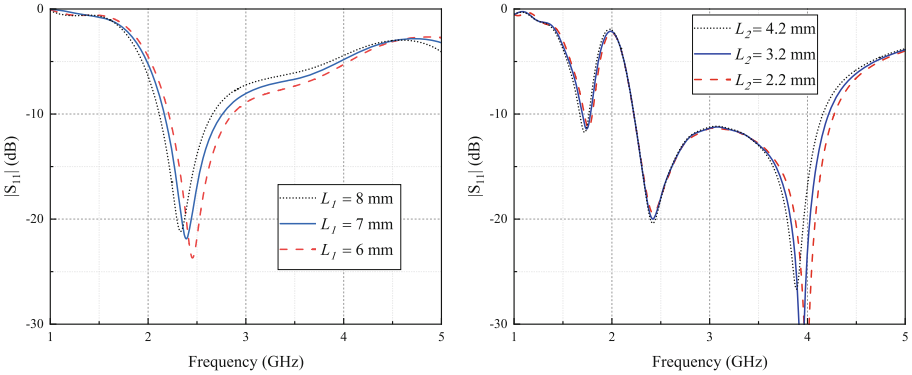

Fig. 7. The parameter variation: (a) L_1; (b) L_2.

3.1 The Effects of Antenna Configuration

The dual-band antenna design was realized by combining two meander-line segments of corresponding lengths each responsible for a respective frequency. L_{f_1} and L_{f_2} were varied to observe the effect on antenna performance at resonant frequencies of $f_1 = 2.4$ GHz and $f_2 = 1.74$ GHz, respectively, as it was dependent on the meander-line length. Figure 7(a) depicts the length variation of the first line path (L_{f_1}) and its effect on the resonant frequency that should correspond to f_1. L_{f_1} was varied by incrementing the stub (L_1) from 3.2 mm to 4.2 mm to monitor the change in the desired first resonance. It can be seen that increasing the line segment's length results in the lower resonant f_1. Similarly, Fig. 7(b) demonstrates the L_{f_2} line segment length variation and its effect on

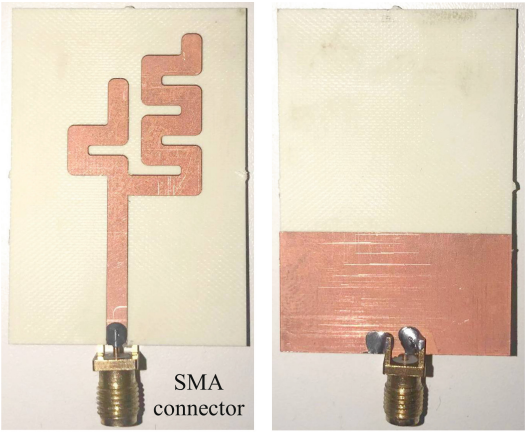

Fig. 8. The fabricated antenna: (a) top view (b) bottom view.

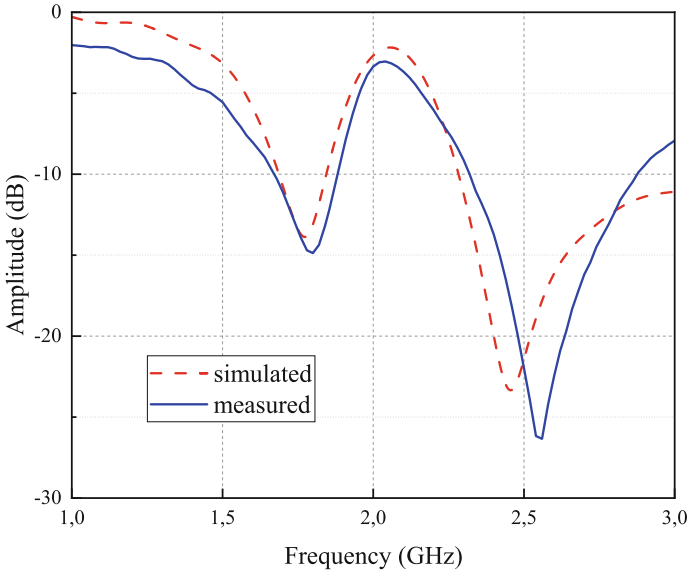

Fig. 9. The obtained results: S_{11} vs frequency.

second resonant frequency. The stub L_2 length was modified from 6 mm to 8 mm to increase the total line segment L_{f_2}, and it is observed that the second resonant frequency f_2 shifts toward the lower value. Finally, the lengths of the line segments were optimized to obtain resonances at f_1 and f_2. The radiation pattern is depicted in Fig. 6. The antenna gain reached 2.1 dBi and 2.6 dBi for 1.74 GHz and 2.4 GHz, accordingly, which are the characteristic gains of meander-line structured antennas.

4 Results and Discussion

To validate the simulation results, the antenna design was fabricated by the LPKF prototyping machine on the RO4350B substrate of thickness 1.54 mm which is shown in Fig. 8. The 50-Ω SMA (SubMiniature Version A) connector was soldered to the feed line. The fabricated antenna's return loss was measured by a vector network analyzer (PNA-X, N5247B).

Figure 9 shows the simulated and experimentally measured S_{11} of the meander-line patch antenna. The measured S_{11} is in good correspondence with the simulation results having a slight deviation on a first resonance. This difference in f_1 is due to the losses at higher frequencies. The discrepancy is accountable as a result of the machine precision during the fabrication and SMA connector soldering. Despite the deviation f_1, that remains within -10 dB bandwidth, the fabricated antenna is feasible to operate in the Wi-Fi band. The validation of the design has demonstrated that the realized dual-band antenna prototype is applicable for RF EH at 1.74 GHz and 2.4 GHz.

5 Conclusion

The abundance of unused EM waves in the urban environment can be conveniently exploited for charging multiple IoT sensor nodes and to enable their independent functionality. Therefore, this paper investigated and analyzed the spectrum and power levels of present RF energy on the university campus. The campus grounds was a suitable location as a general scenario for a public place with many users and expected to have active frequency bands to choose from. The spectrum measurements inferred two potential frequency bands eligible for RF EH and based on that the meander-line microstrip-fed patch antenna is realized. The resonant frequencies were tuned by finding optimal parametric values of meander lines. The antenna has dimensions (in mm) 50×35 and is optimized to operate on 1.74 GHz and 2.4 GHz.

References

1. Gu, X., et al.: Dynamic ambient RF energy density measurements of Montreal for battery-free IoT sensor network planning. IEEE Internet Things J. **8**(17), 13209–13221 (2021)
2. Dautov, K. et al.: Quantifying the impact of slow wave factor on closed-loop defect-based WPT systems. In: IEEE Transactions on Instrumentation and Measurement, vol. 71, pp. 1–10 (2022)
3. Dhungana. A., Bulut, E.: Opportunistic wireless crowd charging of IoT devices from smartphones. In: 16th International Conference on Distributed Computing in Sensor Systems (DCOSS), pp. 376–380 (2020)
4. Toro, U.S., Wu, K., Leung V.C M.: Backscatter Wireless Communications and Sensing in Green Internet of Things. In: IEEE Transactions on Green Communications and Networking, vol. 6, no. 1, pp. 37–55 (2022)

5. Nauryzbayev, G., Abdallah, M., Rabie, K. M.: Outage Probability of the EH-Based Full-Duplex AF and DF Relaying Systems in $\alpha - \mu$ Environment. In: 2018 IEEE 88th Vehicular Technology Conference (VTC-Fall), pp. 1–6 (2018)
6. Raghavandaar, M. et al.: Energy harvesting using 2.45 GHz rectenna for powering sensors in IoT devices. In: International Conference on Electronics, Information, and Communication, pp. 1–3 (2020)
7. Dautov, K. et al.: Analysis and experimental validation of circularly slotted near-field WPT systems. In: 2021 IEEE International Midwest Symposium on Circuits and Systems (MWSCAS), pp. 263–266 (2021)
8. Nauryzbayev, G. et al.: Ergodic capacity analysis of wireless powered AF relaying systems over alpha-μ Fading Channels. In: GLOBECOM 2017–2017 IEEE Global Communications Conference, pp. 1–6 (2017)
9. Vu, H.S. et al.: Multiband ambient RF energy harvesting for autonomous IoT devices. In: IEEE Microwave and Wireless Components Letters, vol. 30, no. 12, pp. 1189–1192 (2020)
10. Ruchi et al.: A rectenna for RF energy harvesting for application in powering IoT device. In: IEEE Wireless Antenna and Microwave Symposium (WAMS), pp. 1–4 (2022)
11. Kwan, J.C., Fapojuwo, A.O.: Measurement and analysis of available ambient radio frequency energy for wireless energy harvesting. In: 2016 IEEE 84th Vehicular Technology Conference, pp. 1–6 (2016)
12. Pinuela, M., Mitcheson, P.D., Lucyszyn, S.: Ambient RF energy harvesting in urban and semi-urban environments. IEEE Trans. Microw. Theory Techn. **61**(7), 2715–2726 (2013)
13. Andrenko, A.S., Lin, X., Zeng, M.: Outdoor RF spectral survey: a roadmap for ambient RF energy harvesting. In: TENCON 2015–2015 IEEE Region 10 Conference, pp. 1–4 (2015)
14. Bhatt, K. et al.: Highly efficient 2.4 and 5.8 GHz dual-band rectenna for energy harvesting applications. In: IEEE Antennas and Wireless Propagation Letters, vol. 18, no. 12, pp. 2637–2641 (2019)
15. Wong, K. et al.: Very-low-profile grounded coplanar waveguide-fed dual-band WLAN slot antenna for on-body antenna application. In: IEEE Antennas and Wireless Propagation Letters, vol. 19, no. 1, pp. 213–217 (2020)
16. Yadav, M. et al.: Gain enhanced dual band antenna backed by dual band AMC surface for wireless body area network applications. In: 2021 IEEE Indian Conference on Antennas and Propagation, pp. 494–497 (2021)
17. Boursianis, A.D., et al.: Multiband patch antenna design using nature-inspired optimization method. IEEE Open J. Antenn. Propag. **2**, 151–162 (2021)